processes

MDPI

Article

Implications of Wettability and Pore Size Superposition on Nanoconfinement Effects for Unconventional Oil and Gas Development Using Mesoporous Zeolites

Shixun Bai [1,*], Jiahui Liu [1], Lu Wang [2] and Rui Jian [1]

[1] School of Petroleum, China University of Petroleum-Beijing at Karamay, Karamay 834000, China; 2024216866@st.supk.edu.cn (J.L.); 2025216870@st.cupk.edu.cn (R.J.)
[2] CNPC Economics & Technology Research Institute, Beijing 100007, China; wanglu689@cnpc.com.cn
* Correspondence: baisxun@cupk.edu.cn

Abstract

The nanoconfinement effect is crucial in unconventional oil and gas development, yet the regulatory mechanism of wettability on it remains unclear. In this study, three SBA type molecular sieves with different pore sizes were used as model materials. Isothermal adsorption experiments were conducted using a BET analyzer, and pore size distributions were determined using the BET method and the DFT method, to systematically investigate the influence of wettability on the nanoconfinement effect. The results show that SBA molecular sieves with different pore sizes exhibit significantly different propane adsorption behaviors. SBA-15-4.2 with smaller pore sizes undergo capillary condensation at lower pressures, while SBA-15 and SBA-15-18 with larger pore sizes require higher pressures. The pore size distribution of the mixed SBA molecular sieve system exhibits a weighted superposition characteristic of the individual material pore size distributions, with each material contributing differently in different pore size ranges. Wettability significantly affects gas adsorption, diffusion, and condensation processes: unmodified SBA molecular sieves are highly hydrophilic and unfavorable for propane adsorption; shale pore surfaces have complex wettability and exhibit unique adsorption preferences for propane. After hydrophobic modification, the isothermal adsorption curve of the oil-wet SBA composite system is closer to that of shale, and the shale isothermal adsorption curve can be well fitted by adjusting the proportion of SBA molecular sieves in the mixture. This study provides a theoretical basis and experimental means for understanding the production mechanisms of unconventional reservoirs and optimizing production technologies.

Keywords: nanoconfinement effect; wettability; SBA molecular sieve; isothermal adsorption; shale oil and gas development

Academic Editor: Dicho Stratiev

Received: 2 June 2026
Revised: 20 June 2026
Accepted: 24 June 2026
Published: 26 June 2026

1. Introduction

Large-scale development of unconventional oil and gas resources, such as shale oil [1] and shale gas [2], has become a strategic choice to ensure energy security [3,4]. However, the development of these resources is complicated by the prevalence of the nanoconfinement effect [5]. In the confined pore spaces of such reservoirs, substances exhibit unique physicochemical property changes due to nanoscale confinement [6]. This effect enhances the interaction between gas molecules and pore walls while the restricted intermolecular distance leads to changes in adsorption thermodynamic and kinetic behaviors [7,8].

The nanoconfinement effect fundamentally alters fluid behavior in several ways. Studies have shown that gas adsorption capacity can significantly increase under nanoconfinement, while diffusion rates decrease by 1–2 orders of magnitude and adsorption isotherms exhibit non-classical characteristics [6]. Phase transition behavior also shifts significantly. For example, the liquefaction temperature of methane in 2 nm pores can be 15–20 K lower than under macroscopic conditions [6]. Consequently, while nanopores can substantially increase gas adsorption storage capacity, the nanoconfinement effect also makes gas more difficult to desorb during production [9–11]. This effect determines the occurrence state and flow patterns of shale oil and gas, directly affecting the accuracy of reserve estimation and the effectiveness of development strategies [12].

A critical factor in regulating the nanoconfinement effect is wettability, a core parameter of solid surface-fluid interaction. Wettability, typically quantified by contact angle, is essentially a comprehensive manifestation of solid surface energy and fluid interfacial tension [13]. In the nanopore network of shale reservoirs, fluid behavior is strongly coupled by the interaction between pore wall and gas molecules [14,15]. The reduction in pore size leads to a significant increase in the van der Waals interactions between fluid molecules and the pore wall, causing phase diagram shifts and anomalous phase transition behavior [16,17]. In nanopores, hydrophilic surfaces enhance the oriented adsorption of polar molecules (such as water and CO_2) through hydrogen bonding and dipole interactions, forming ordered interface layers, while hydrophobic surfaces promote the adsorption and enrichment of non-polar molecules (such as CH_4 and C_2H_6) through dispersion forces [18].

The regulatory role of wettability on the nanoconfinement effect is multifaceted. It directly affects molecular arrangement structure, interface layer thickness, and phase transition critical points by changing the fluid-wall interaction energy, thereby reshaping the manifestation of the nanoconfinement effect [6]. For instance, Song et al. found that as the pore radius decreases from 100 nm to 10 nm, the minimum miscibility pressure of shale oil and CO_2 decreases by more than 20%, revealing the regulatory effect of interfacial tension reduction on phase behavior [7]. Furthermore, wettability changes the energy barrier at the interface, affecting phase transition kinetics. Hydrophobic surfaces lower the fluid saturation pressure, making the gas phase easier to form during desorption, whereas hydrophilic surfaces increase the saturation pressure by enhancing interfacial binding energy, inhibiting the vaporization process [19,20].

The influence of wettability extends to adsorption selectivity and transport mechanisms. The high specific surface area of nanopores makes adsorption the primary form of fluid occurrence [21]. Xu et al. confirmed through molecular simulation that methane exhibits preferential adsorption in kerogen nanopores, while hydrogen is uniformly distributed due to weak wall interaction forces, demonstrating the decisive influence of molecular-wall interactions on adsorption selectivity [22]. Li et al. showed through isothermal adsorption experiments that the adsorption capacity of CO_2 in hydrophilic mesoporous materials increases linearly with pressure, while CH_4 in hydrophobic pores exhibits non-linear adsorption characteristics, confirming the decisive influence of wettability on adsorption patterns [6]. Moreover, the classical Darcy's law fails at the nanoscale, where fluids exhibit non-classical transport modes such as slip flow and diffusion flow [23]. Zhang et al. found that the micro-nano confinement effect reduces crude oil viscosity by 30–50%, significantly improving CO_2 flooding efficiency [24]. Additionally, Feng et al. found that hydrophobic surfaces can delay gas–liquid separation, while hydrophilic surfaces accelerate phase separation; this difference is directly related to the core need for fluid phase behavior control in shale oil and gas development [19]. The contact angle magnitude also determines the fluid slip at the pore wall, where hydrophilic pore walls lead to reduced fluid slip length and increased flow resistance, while hydrophobic surfaces

can result in significant slip and lower the threshold pressure to initiate flow within the porous media [25].

Despite the progress, current understanding of wettability and the nanoconfinement effect has several limitations. First, experimental models are often oversimplified. Mesoporous materials (such as SBA [26]) were mainly used to achieve wettability regulation through surface modification; however, there is a lack of composite interfaces of organic and inorganic matter in shale and multimodal pore size distributions [27]. Second, multifactor coupling analysis is insufficient. In actual reservoirs, wettability has strong coupling with pore structure, fluid composition, and temperature-pressure conditions [28]. Jia et al. pointed out that when CO_2 is injected into shale oil reservoirs, the non-equilibrium phase behavior in nanopores is correlated with macroscopic seepage, and traditional single-factor analysis cannot reveal its intrinsic mechanism [29]. Third, the adaptability of theoretical models is insufficient. Model parameters based on DFT (density functional theory) or MD (molecular dynamics) are difficult to accurately map to real shale systems [30]. For example, the shale oil-CO_2 phase behavior model constructed by Song has a prediction error exceeding 15% when applied to natural shale [31].

To bridge these gaps, this study systematically measures the adsorption isotherms of N_2 and C_3H_8 in nanopores with different wettability through isothermal adsorption experiments. Furthermore, shale simulation method was developed based on molecular sieve composites to construct a mixed wettability model system with a multimodal pore size distribution.

2. Materials and Methods

2.1. Materials and Equipment

Silica molecular sieves SBA-15, SBA-15-18, and SBA-15-4.2 were all purchased from Nanjing Jicang Nano Technology Co., Ltd. (Nanjing, China) Ethanol (95%), ammonia solution (35%), methacryloxypropyltrimethoxysilane (KH-570) were procured from Shanghai Macklin Biochemical Technology Co., Ltd. (Shanghai, China) High-purity nitrogen (99.999%), liquid nitrogen, and a propane-helium mixture were also utilized. The BET analyses and adsorption heat analyses were conducted using the Surface Area and Pore Size Analyzer from Quantachrome Instruments (Boynton Beach, FL, USA).

2.2. Determination of Pore Size Distribution and Adsorption Heat of SBA Molecular Sieves

Pore size distribution of the SBA materials before and after hydrophobic modification was conducted via the BET analysis and evaluated using the DFT method. Prior to the BET analyses, the samples were dried in a vacuum oven at 120 °C for 12 h to eliminate surface moisture and volatile impurities, and were then transferred to sample tubes and sealed for preservation. High-purity nitrogen served as the adsorbate, with liquid nitrogen providing the experimental temperature. Approximately 0.5 g of the SBA samples was added to the sample tube. Under vacuum conditions, the sample was heated to 120 °C and degassed for 6 h to remove surface adsorbates. The sample tube was then immersed in a liquid nitrogen bath, maintaining a temperature of −196.15 °C (77 K). Nitrogen gas was introduced incrementally, adjusting the relative pressure (P/P_0) range from 0.05 to 0.35, and the equilibrium adsorption amount at each point was recorded. Multiple points were tested continuously until the adsorption amount approached saturation. The adsorption amounts at various relative pressures were plotted against the relative pressure into the nitrogen adsorption isotherms. The linear portion of the adsorption isotherm was selected, and the BET equation was utilized to fit the data and calculate the specific surface area. Based on the adsorption branch data, the DFT model was employed to compute the pore size distribution (PSD). To determine the change in wettability before and after the

hydrophobic modification, propane gas was used as the adsorbate following the above procedure at 0 °C (273.15 K). The adsorption heat was directly exported from the built-in software.

2.3. Hydrophobic Modification of SBA Materials by KH-570

KH-570 (methacryloxypropyltrimethoxysilane) features an inorganic-philic siloxy group at one end and an organic-philic methacryloxy group at the other [32]. When KH-570 reacts with silica molecular sieves, the siloxy groups interact with the abundant hydroxyl groups on the silica surface, undergoing a dehydration condensation reaction to establish stable covalent bonds. The introduction of polar groups by KH-570 causes the modified surface to repel non-polar molecules [33]. To graft the SBA materials with KH-570, 3.6 g of ammonia water and 10.8 g of water were added into a 50 mL test tube vial. Subsequently, 2 g of molecular sieve was weighed and introduced into the vial. After shaking, the vial was placed in an oven to preheat for 10 min at 110 °C. The vial was then removed, and 5.4 g of KH-570 was added. Following uniform shaking, it was returned to the oven and heated for 40 min at a temperature of 120 °C. After heating, the vial was allowed to stand, the separated liquid layer was removed, and alcohol was added for rinsing. Finally, the vial was placed in an oven and dried at a 80 °C, yielding the KH-570 modified molecular sieves.

3. Results and Discussion

3.1. Pore Size Distribution Patterns of SBA Molecular Sieve Mixed Systems

According to existing literature [34], when molecular sieve materials with different pore sizes are mixed, their pore size distribution can be regarded as the weighted superposition of the individual material pore size distributions. Let the mass fractions of each molecular sieve material in the mixed system be ω_1, ω_2, ω_3 (corresponding to SBA-15, SBA-15-4.2, SBA-15-18), and their respective pore size distribution functions be $f_1(r)$, $f_2(r)$, $f_3(r)$; then the pore size distribution function of the mixed system can be expressed as:

$$f(r) = \omega_1 f_1(r) + \omega_2 f_2(r) + \omega_3 f_3(r) \quad (1)$$

The pore distribution of the mixed system at a certain pore size is obtained by weighted summation of the pore distributions of each individual material at that pore size according to their mass fractions. SBA-4.2 has a mean pore size of 4.2 nm and contributes significantly in the small pore size range; SBA-15 has a pore size of 6–11 nm and mainly affects the medium pore size range, and SBA-15-18 has a pore size of 15–20 nm and dominates the characteristics of the large pore size range.

During the experiment, the pore size distribution of each material was first measured individually (shown in Figure 1), then they were mixed at a ratio of 2:4:4. The mixing process employed a combination of mechanical stirring and ultrasonic dispersion, during which the materials were first stirred at a fixed speed in a mechanical stirrer for preliminary mixing, then transferred to an ultrasonic disperser for further dispersion to ensure full contact and uniform mixing.

Experimental results shown in Figure 2 show that the pore size distribution of the mixed system obtained by the DFT method exhibits, to a certain extent, the superposition characteristics of the individual material pore size distributions.

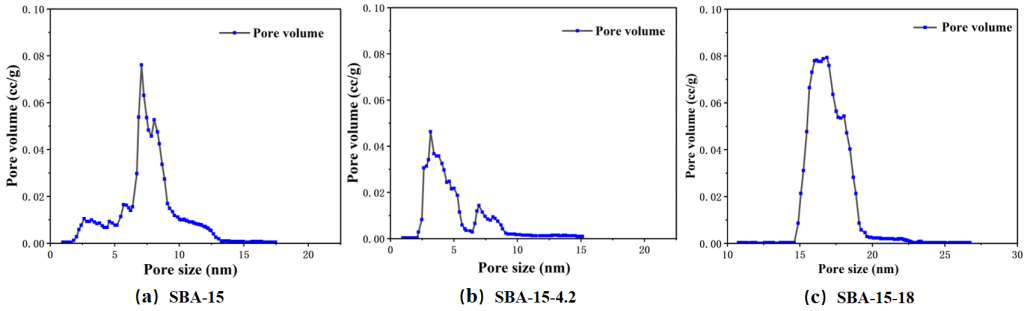

Figure 1. Pore size distribution of (**a**) SBA-15, (**b**) SBA-15-4.2, and (**c**) SBA-15-18.

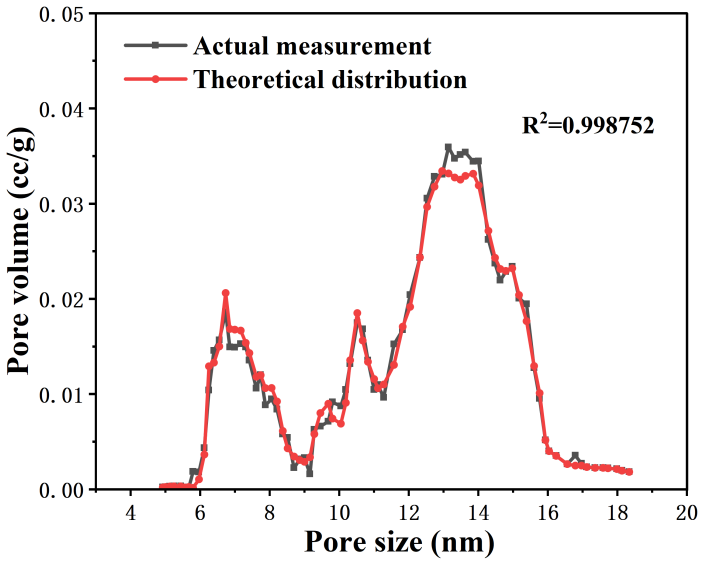

Figure 2. Comparison between the theoretical pore size distribution (fitted curve) of the molecular sieve mixture via superposition by mass fraction and the actual pore size distribution (experimental data) of the mixture.

To verify the superposition property of pore size distribution, regression fitting was performed using the least squares method to determine the weighting coefficients. Let the pore volume proportions of SBA-15, SBA-15-4.2, and SBA-15-18 in this range be x_1, x_2, x_3, respectively, and the pore volume proportion of the mixed system in this range be y. Assuming the weighting equation is:

$$y = a_1x_1 + a_2x_2 + a_3x_3 \quad (2)$$

Using the least squares method to minimize

$$\sum(y_i - (a_1x_{1i} + a_2x_{2i} + a_3x_{3i}))^2 \quad (3)$$

The results give a_1 = 0.22, a_2 = 0.39, and a_3 = 0.39, with a ratio of approximately 2:4:4, leading to an R^2 value of over 0.99. The fitted weighting coefficients are relatively close to the actual proportion coefficients. As the mixing process was purely physical, the fluctuations were likely due to weighing inaccuracies and mixing heterogeneities. This verifies that the pore size distribution curves of each SBA material superimposed according to the weighting coefficients can well produce the pore size distribution curve of the mixture, demonstrating the superposition property of pore size distribution curves.

3.2. Propane Isothermal Adsorption Characteristics

Isothermal adsorption curves [35,36] are an important basis for studying the propane adsorption characteristics of SBA molecular sieves with different pore sizes. According to the BDDT classification [37], isothermal adsorption curves have multiple types: Type I corresponds to monolayer adsorption or microporous materials; Type II corresponds to non-porous or macroporous solids; Type IV corresponds to mesoporous materials. The smaller the pore size, the stronger the constraining effect of the internal nanoconfinement environment on gas molecules. The pore size of SBA-15-4.2 is in the smaller range, and the spatial constraint on gas molecules is more significant. Under this strong confinement environment, the interactions between gas molecules and between gas molecules and pore walls are enhanced. As the pressure gradually increases, gas molecules more easily accumulate in smaller pores and reach higher concentrations, thereby satisfying the conditions for nano-condensation at relatively low pressures, i.e., the transition from gas to liquid occurs. However, due to the hydrophilic nature of the SBA material (silica-based), the interactions between the propane and the pore walls are relatively weak; therefore, the isothermal adsorption curves of the SBA materials only show vague inflection points (Figure 3), indicating weak nanoconfinement effects.

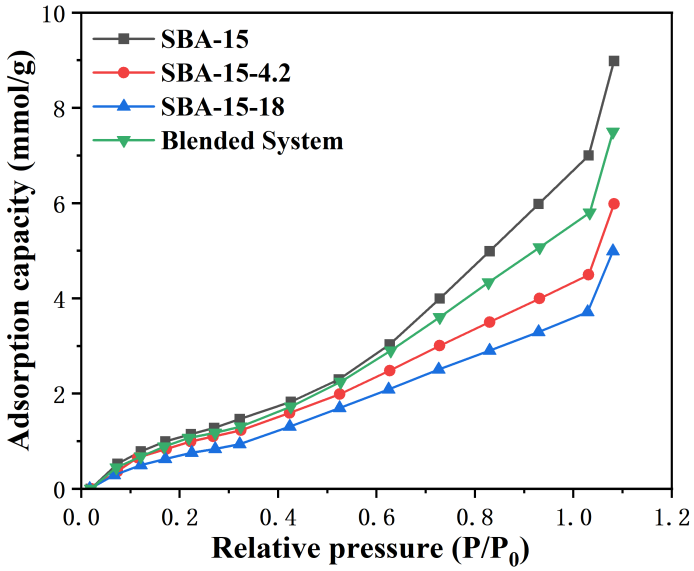

Figure 3. Comparison between the isotherm adsorption curves of SBA-15, SBA-15-4.2, SBA-15-18 and that of their mixture (blended system).

When these SBA molecular sieves are mixed, the overall isothermal adsorption curve presents a relatively smooth shape without obvious steep slopes. This is because the isothermal adsorption curves of each individual SBA molecular sieve superimpose on each other. Taking the composite of SBA-15, SBA-15-4.2, and SBA-15-18 at a mass ratio of 1:1:1 as an example, during the isothermal adsorption process, molecular sieves with different pore sizes each contribute to the overall adsorption curve. From a mathematical perspective, the isothermal adsorption curve of the composite system is a superposition of each individual curve according to the weights. If the adsorption capacities of each individual molecular sieve are expressed as $Q_1(P)$, $Q_2(P)$, and $_3(P)$, the adsorption capacity of the composite system can be expressed as:

$$Q_{tot}(P) = \omega_1 Q_1(P) + \omega_2 Q_2(P) + \omega_3 Q_3(P) \quad (4)$$

where ω_1, ω_2, and ω_3 are the mass fractions of each molecular sieve, respectively. Fitting analysis found that the key coefficients describing this superposition relationship are rela-

tively close to the actual proportions of each molecular sieve (1:1:1), strongly demonstrating the superposition property of the adsorption characteristics of the mixed system.

The above phenomena indicate that in the composite system, not only does a superposition relationship exist in terms of pore size, but the nanoconfinement effect also exhibits a superposition relationship.

3.3. Influence of Wettability on the Nanoconfinement Effect

Unmodified SBA molecular sieves and shale differ greatly in wettability, which affects their propane adsorption capacity. From the perspective of surface chemical properties, the surface of unmodified SBA molecular sieves is mainly composed of silanol groups and is highly hydrophilic; while shale pore surfaces contain abundant organic matter and clay minerals, with more complex wettability that includes both hydrophilic and oleophilic properties, and some regions may also exhibit intermediate wettability. This fundamental difference in wettability makes the adsorption forces, adsorption selectivity, and nanoconfinement effects of the two toward propane molecules vastly different.

At the microscopic level, the surface of unmodified SBA molecular sieves is hydrophilic, and there is only weak van der Waals force between it and non-polar propane molecules, making it difficult for propane molecules to adsorb stably. In contrast, shale pore surfaces have complex wettability, and propane molecules may form stronger interactions with the surface in the oil-wet regions. Therefore, unmodified SBA molecular sieves have no specificity for propane adsorption, while shale pores exhibit specific adsorption preferences for propane molecules based on their own wettability and pore structure. The isothermal adsorption curve on a shale sample for propane is shown in Figure 4.

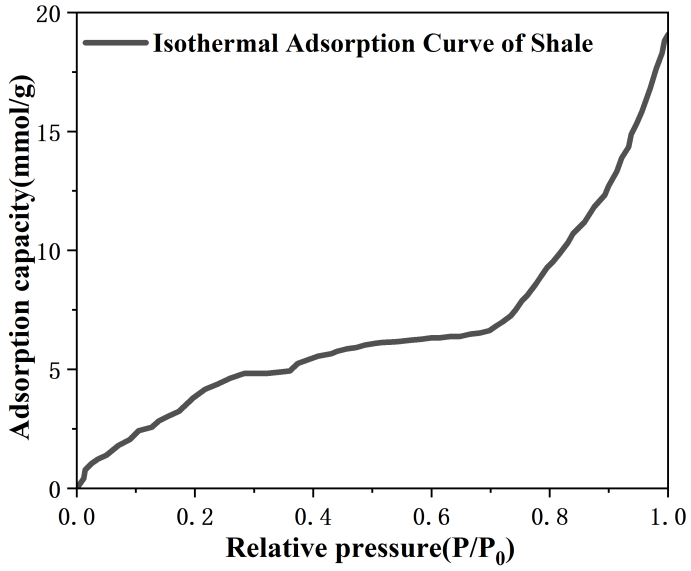

Figure 4. Isothermal propane adsorption curve for a shale sample.

From the isothermal adsorption curves (Figures 3 and 4), it can be seen that the propane adsorption curve of the unmodified SBA molecular sieve composite system differs greatly from the adsorption curve of shale. This difference is manifested not only in adsorption capacity but also in the shape and slope of the curves. The adsorption curve of shale typically has multi-segment characteristics, indicating the existence of multiple wettability and adsorption mechanisms within its pores, while the adsorption curve of unmodified SBA molecular sieves is relatively simple and cannot truly reflect the complex adsorption process in shale pores. Therefore, surface modification of SBA molecular sieves is needed to

match their wettability with shale in order to accurately simulate the adsorption behavior of shale gas.

3.4. Adsorption Behavior of Hydrophobically Modified SBA Composite System

To improve the similarity between the composite system and shale adsorption characteristics, hydrophobic modification using KH-570 was conducted to transform the SBA materials into an oil-wet state. As direct contact angle measurement was challenging on a powder material such as SBA, adsorption heat was quantified instead as a measure of wettability, with higher adsorption heat between an organic gas and the solid surface indicating higher extent of oil-wetness. The adsorption heat of propane on the SBA materials during the adsorption process is compared in Figure 5. It is evident that the adsorption heat for all materials increased post-modification, suggesting stronger affinity between the molecular sieve surfaces and propane. This can be regarded as proof that the SBA materials become more oil-wet due to KH-570 treatment.

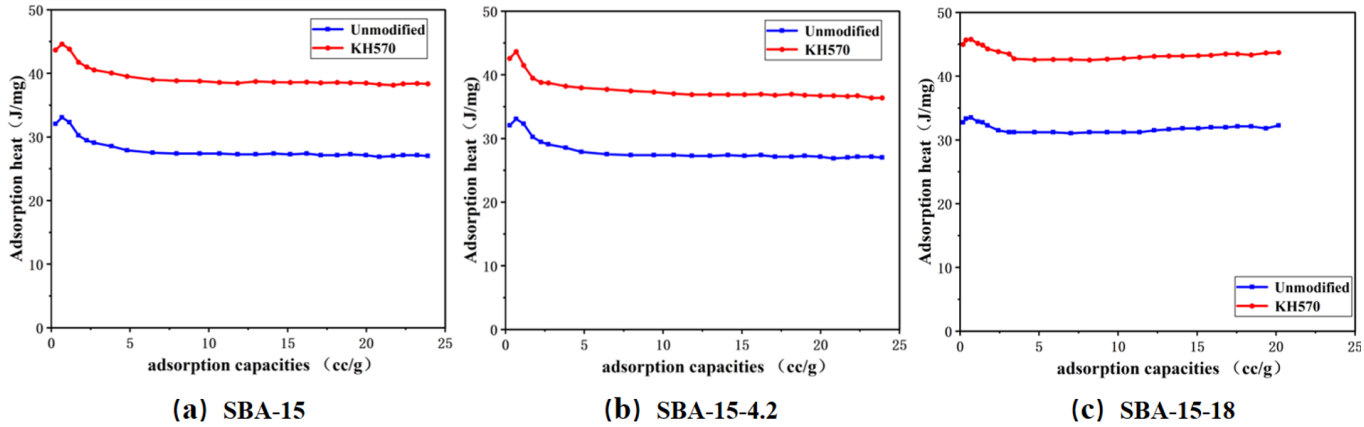

Figure 5. Comparison of adsorption heat between propane and (**a**) SBA-15, (**b**) SBA-15-4.2, and (**c**) SBA-15-18 before and after hydrophobic modification by KH-570

A least squares optimization model was employed to determine the mixing ratio of the SBA materials, minimizing the mean squared error (MSE) between the pore size distribution after compositing and the shale pore size distribution to solve for the optimal ratio:

$$min \sum [\omega_1 f_1(x_i) + \omega_2 f_2(x_i) + \omega_3 f_3(x_i) - f_{shale}(x_i)]^2 \quad (5)$$

The constraint conditions are $\omega_1 + \omega_2 + \omega_3 = 1$ and $\omega_i > 0$ (i = 1, 2, 3), solved using the fmincon function in MATLAB (Version R2024a) to be approximately 0.3, 0.3, and 0.4.

Experimental results show (Figure 6) that the isothermal adsorption curve of the oil-wet SBA composite system is closer to the isothermal adsorption curve of shale. This result fully demonstrates the important influence of wettability on phase behavior [38]. The change in wettability affects the adsorption, diffusion, and condensation processes of gas molecules on the material surface and within the pores. In the oil-wet environment, the interaction between gas molecules and the material surface is more similar to that in shale pores, making the adsorption capacity, adsorption selectivity, and nanoconfinement effect more similar to those of shale.

Compared with the unmodified SBA mixture, the isothermal adsorption curve shape of the modified SBA mixture for propane is closer to that of shale with a similar pore size distribution, but not completely overlapping. The reason is that the degree and uniformity of modification of SBA by the selected silane coupling agent may not be completely consistent with shale, but the fact that the result is close to shale further proves the key role of wettability in regulating adsorption phase behavior. This method of SBA molecular

sieve modification and mixing can facilitate the studies on hydrocarbon phase transitions in unconventional reservoirs by simulating the pore size and wettability of shale and using composite systems of SBA molecular sieves with different pore sizes.

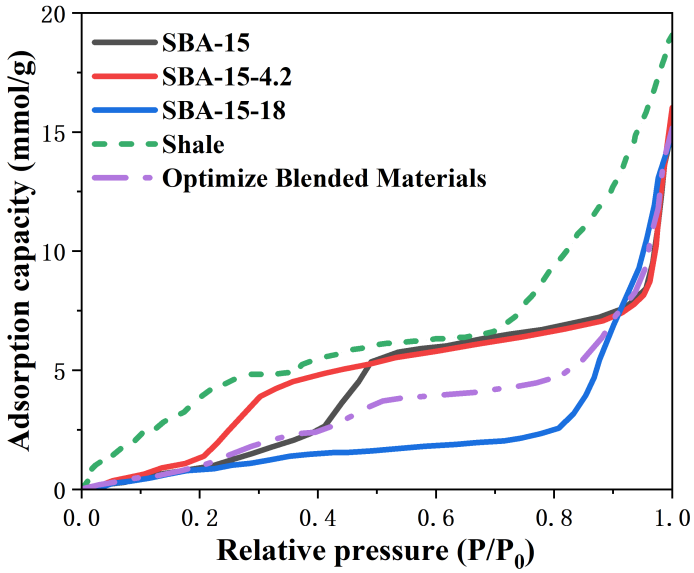

Figure 6. Comparison between the isotherm propane adsorption curves for SBA-15, SBA-15-4.2, SBA-15-18, their mixture, the shale sample.

4. Conclusions

This study systematically investigated the influence of wettability on the nanoconfinement effect using SBA-type molecular sieves as model porous media. By comparing unmodified hydrophilic surfaces with hydrophobically modified oleophilic surfaces, the following conclusions are drawn:

(1) The pore size distribution of the mixed SBA molecular sieve system exhibits superposition characteristics of the individual materials. This characteristic provides an important reference for simulating shale pore structure and studying gas adsorption and diffusion in unconventional reservoirs.

(2) SBA molecular sieves can be hydrophobically modified using silane coupling agent KH-570, leading to increased adsorption heat of propane, and therefore greater oil-wetness on modified SBA materials.

(3) After hydrophobic modification of SBA molecular sieves, the isothermal adsorption curve of the oil-wet SBA composite system is closer to that of shale, further proving the key role of wettability in regulating adsorption phase behavior. This provides an effective experimental method for studying gas adsorption in shale gas reservoirs and helps to more accurately understand the production mechanisms of unconventional reservoirs.

These findings provide not only a theoretical basis for understanding the occurrence state of shale oil and gas but also an effective experimental methodology for simulating nanoconfinement effects under reservoir conditions.

Author Contributions: Conceptualization, S.B.; methodology, J.L.; Experiment, J.L. and R.J.; writing—original draft preparation, review and editing, L.W. and S.B. All authors have read and agreed to the published version of the manuscript.

Funding: This work has been funded by the Natural Science Foundation of Xinjiang Uygur Autonomous Region (No. 2023D01B09) and the Regional Fund of the National Natural Science Foundation of China (No. 52464002).

Data Availability Statement: The original contributions presented in this study are included in the article. Further inquiries can be directed to the corresponding author.

Conflicts of Interest: Author Lu Wang was employed by CNPC Economics & Technology Research Institute. The remaining authors declare that the research was conducted in the absence of any commercial or financial relationships that could be construed as a potential conflict of interest. The CNPC Economics & Technology Research Institute had no role in the design of the study; in the collection, analyses, or interpretation of data; in the writing of the manuscript, or in the decision to publish the results.

Abbreviations

The following abbreviations are used in this manuscript:

BET	Brunauer–Emmett–Teller
SBA	Santa Barbara Amorphous
DFT	density functional theory
MD	molecular dynamics
MSE	mean squared error

References

1. Li, Q.; Li, Q.; Wang, F.; Wu, J.; Wang, Y.; Jin, J. Effects of geological and fluid characteristics on the injection filtration of hydraulic fracturing fluid in the wellbores of shale reservoirs: Numerical analysis and mechanism determination. *Processes* **2025**, *13*, 1747. [CrossRef]
2. Li, Q.; Zhao, D.; Yin, J.; Zhou, X.; Li, Y.; Chi, P.; Han, Y.; Ansari, U.; Cheng, Y. Sediment Instability Caused by Gas Production from Hydrate-bearing Sediment in Northern South China Sea by Horizontal Wellbore: Sensitivity Analysis. *Nat. Resour. Res.* **2025**, *34*, 1667–1699. [CrossRef]
3. Song, S.; Yang, E.; Sha, M. Influencing factors of occurrence state of shale oil based on molecular simulation. *Pet. Reserv. Eval. Dev.* **2023**, *13*, 31–38. [CrossRef]
4. Chen, J.; Wang, H.; Chen, X.; Tang, Y.; Tang, L.; Si, R.; Wang, H.; Huang, X.; Leng, B. Study on main controlling factors of CO_2 huff-n-puff for enhanced oil recovery and storage in shale oil reservoirs. *Pet. Reserv. Eval. Dev.* **2023**, *15*, 537–544. [CrossRef]
5. Wang, Y.; Zhao, F.; Huang, S.; Sun, H.; Yang, C.; Bi, S. Adaptability of CO_2 Huff and Puff in Shale Oil Considering Nano Confinement Effect. *Oilfield Chem.* **2024**, *41*, 498–504+542. [CrossRef]
6. Li, M.; Sun, M.; Mohammadian, E.; Ji, Y.; Blach, T.P.; Ostadhassan, M.; Wen, J.; Wu, C.; Pan, Z. Confinement effect in nanopores of shale and coal reservoirs: A review on experimental characterization methods. *Gas Sci. Eng.* **2024**, *123*, 205249. [CrossRef]
7. Song, Z.; Deng, S.; Song, Y.; Liu, Y.; Xian, C.; Zhang, J.; Han, X.; Cao, S.; Fu, L.; Cui, H. High-pressure phase behavior and mass transfer law of Gulong shale oil and CO_2 in Daqing oilfield. *Acta Pet. Sin.* **2024**, *45*, 390–402. [CrossRef]
8. Xing, X.; Feng, Q.; Zhang, W.; Wang, S. Phase behavior of methane in shale inorganic nanopores using Monte Carlo molecular simulation. *J. Nat. Gas Sci. Eng.* **2022**, *105*, 104691. [CrossRef]
9. Guo, Y.; Shi, J.; Qiu, J.; Xu, Z.; Bao, B. Visualized investigation of transport and phase behaviors during CO_2 huff-n-puff in nanomatrix-fracture tight formations. *Fuel* **2023**, *354*, 129344. [CrossRef]
10. Weifeng, L. Phase Behavior of High-Viscosity Oil and Tuning of Rock Wettability Within Porous Media. Ph.D. Thesis, Nanjing University, Nanjing, China, 2020. [CrossRef]
11. Zhan, S.; Bao, J.; Wang, X.; Wang, W.; Su, Y.; Zhang, M.; Wang, Y.; Jin, Z. A comparative study of shale oil transport behavior in graphene and kerogen nanopores with various roughness via molecular dynamics simulations. *Chem. Eng. J.* **2024**, *498*, 155173. [CrossRef]
12. Liu, B.; Lei, X.; Feng, D.; Ahmadi, M.; Wei, Z.; Chen, Z.; Jiang, L. Nanoconfinement effect on the miscible behaviors of CO_2/shale oil/surfactant systems in nanopores: Implications for CO_2 sequestration and enhanced oil recovery. *Sep. Purif. Technol.* **2025**, *356*, 129826. [CrossRef]
13. Qiu, X.; Liu, Y.; Zheng, S.; Yang, H. Molecular insights into the composition distribution and phase behavior of hydrocarbon mixtures in a multiscale system with mixed wettability. *Int. J. Hydrogen Energy* **2025**, *109*, 648–659. [CrossRef]
14. Miscevic, M.; Lavieille, P.; Pilaud, B. Numerical study of convective flow with condensation of a pure fluid in capillary regime. *Int. J. Heat Mass Transf.* **2009**, *52*, 5130–5140. [CrossRef]
15. Sodagar-Abardeh, J.; Loimer, T. Description of confined nanoflow transport considering the effects of capillary condensation and heat transfer by means of a two-phase lattice Boltzmann model. *Chem. Eng. Sci.* **2025**, *316*, 121935. [CrossRef]

16. Wang, Y.; Lei, Z.; Liu, Y.; Pan, X.; Chen, Z.; Zhang, Y.; Zheng, X.; Liu, P.; Han, y. Phase behavior of CO_2-shale oil in nanopores. *Pet. Explor. Dev.* **2025**, *52*, 182–195. [CrossRef]
17. Kalam, S.; Arif, M.; Raza, A.; Lashari, N.; Mahmoud, M. Data-driven modeling to predict adsorption of hydrogen on shale kerogen: Implication for underground hydrogen storage. *Int. J. Coal Geol.* **2023**, *280*, 104386. [CrossRef]
18. Argüelles-Vivas, F.J.; Abeykoon, G.A.; Okuno, R. Wettability modifiers for enhanced oil recovery from tight and shale reservoirs. In *Unconventional Shale Gas Development*; Moghanloo, R.G., Ed.; Gulf Professional Publishing: Houston, TX, USA, 2022; pp. 345–391. [CrossRef]
19. Feng, D.; Bakhshian, S.; Wu, K.; Song, Z.; Ren, B.; Li, J.; Hosseini, S.A.; Li, X. Wettability effects on phase behavior and interfacial tension in shale nanopores. *Fuel* **2021**, *290*, 119983. [CrossRef]
20. Kim, C.; Devegowda, D. Molecular dynamics study of fluid-fluid and solid-fluid interactions in mixed-wet shale pores. *Fuel* **2022**, *319*, 123587. [CrossRef]
21. Zhang, M.; Gao, M.; Liu, Z.; Jin, Z. Molecular insights into mass transfer and adsorption behaviors of hydrocarbon and CO_2 in quartz multiple-nanopore system. *Fuel* **2024**, *362*, 130816. [CrossRef]
22. Xu, Z.; Huang, L.; Yang, Q.; Feng, X.; Tian, B.; Chen, Q.; Qiu, X.; Wang, L.; Liu, Y.; Ning, Z.; et al. Coupling effect of fluid molecular structure and nanoporous structure on the confined phase behavior of butane isomers in shale nanopores. *Fuel* **2025**, *379*, 132983. [CrossRef]
23. Zhang, P.; Lu, S.; Li, J.; Wang, J.; Zhang, J. Oil occurrence mechanism in nanoporous shales: A theoretical and experimental study. *Mar. Pet. Geol.* **2023**, *156*, 106422. [CrossRef]
24. Zhang, Y.; Zhang, M.; Liu, R.; Chen, J. Investigation of CO_2 flooding considering the effect of confinement on phase behavior. *Earth Sci. Front.* **2023**, *30*, 306–315. [CrossRef]
25. Yuan, L.; Zhang, Y.; Liu, S.; Zhang, Y.; Chen, C.; Song, Y. Study on the slip behavior of CO_2-crude oil on nanopore surfaces with different wettability. *Int. J. Heat Mass Transf.* **2024**, *218*, 124787. [CrossRef]
26. Zhu, J.; Shen, J. Adsorption of Basic Nitrogen Compounds From Oil by SBA-15 Zeolite. *Acta Pet. Sin. (Pet. Proccesing Sect.)* **2012**, *28*, 566–570. [CrossRef]
27. Cai, J.; Jiao, X.; Wang, H.; He, W.; Xia, Y. Multiphase fluid-rock interactions and flow behaviors in shale nanopores: A comprehensive review. *Earth-Sci. Rev.* **2024**, *257*, 104884. [CrossRef]
28. Li, B.; Sui, H.; Wang, D.; Wang, Y.; Zhang, F.; Yao, J. Molecular insights into CO_2 enhanced oil recovery and CO_2 storage in quartz nanopores. *Geoenergy Sci. Eng.* **2025**, *246*, 213640. [CrossRef]
29. Jia, Z.; Cao, R.; Pu, B.; Linsong, C.; Li, P.; Awotunde, A.A.; Lin, Y.; Pan, Q.; Sun, Y. Effects of non-equilibrium phase behavior in nanopores on multi-component transport during CO_2 injection into shale oil reservoir. *Energy* **2024**, *307*, 132614. [CrossRef]
30. Wang, Y.; Jin, Z. Effect of pore size distribution on hydrocarbon mixtures adsorption in shale nanoporous media from engineering density functional theory. *Fuel* **2019**, *254*, 115650. [CrossRef]
31. Yilei, S. Phase Behavior and Flow Mechanisms During CO_2 Injection in Gulong Shale Oil Under Nanoconfinement Effect. Ph.D. Thesis, China University of PEtroleum (Beijing), Beijing, China, 2023. [CrossRef]
32. Xu, Z.; Sun, J.; Liu, J.; Lv, K.; Dong, X.; Wang, Z.; Zhang, T.; Sun, Y.; Dai, Z. Development and performance evaluation of high temperature resistant strong adsorption rigid blocking agent. *Pet. Sci.* **2024**, *21*, 2650–2662. [CrossRef]
33. Zhao, H.; Han, H. Synthesis and characterization of functionalized SBA-15 silica through template removal. *J. Solid State Chem.* **2020**, *282*, 121074. [CrossRef]
34. Jianlin, P. Investigatin on the Effect of Pre-Adsorbed Water on Methane Storage in MCM-41 Molecular Sieve. Ph.D. Thesis, China University of Petroleum (East China), Qingdao, China, 2022. [CrossRef]
35. Yanling, G. Mechanism and Mathematical Model of Gas-Water Transport in Shale. Ph.D. Thesis, China University of Petroleum (Beijing), Beijing, China, 2023. [CrossRef]
36. Yao, H.; Wang, W.; He, X.; Zheng, Y.; Ni, Z. Development practices of geology-engineering integration in complex structural area of Nanchuan normal pressure shale gas field. *Pet. Reserv. Eval. Dev.* **2023**, *13*, 537–547. [CrossRef]
37. Peng, L. Application of Isothermal Adsorption Curve on the Investigation of Pore Structure in Shale. Ph.D. Thesis, Chengdu University of Technology, Chengdu, China, 2016.
38. Zhang, K.; Li, G.; Ma, S.; Wang, L.; Liu, Z.; Liu, Z.; Luo, T.; Zheng, J.; Wu, Z. Molecular dynamics simulations of methane flow behavior in clay and methane hydrate nanopores. *J. Mol. Liq.* **2025**, *424*, 127112. [CrossRef]